Unipolar resistive switching characteristics of room temperature grown SnO_2 thin films

Kazuki Nagashima,[1] Takeshi Yanagida,[1,2,a)] Keisuke Oka,[1] and Tomoji Kawai[1,b)]
[1]*Institute of Scientific and Industrial Research, Osaka University, 8-1 Mihogaoka, Ibaraki, Osaka 567-0047, Japan*
[2]*PRESTO, Japan Science and Technology Agency, 4-1-8 Honcho, Kawaguchi, Saitama 332-0012, Japan*

(Received 2 March 2009; accepted 28 May 2009; published online 18 June 2009)

The resistive switching characteristics of room temperature grown SnO_2 films were investigated by fabricating the metal-oxide-metal sandwich structures. The unipolar operation was found in all devices. Experiments, including the size and material dependencies of the top electrodes and the three terminal device structures, demonstrated the rupture and formation of conducting filaments near the anode. The Ohmic behavior was observed in both on- and off-states when using Au and Ti top electrodes, whereas the Schottky behavior was only found in the off-state for Pt. The analysis on the transport properties indicates the presence of insulative crystalline SnO_2 near the anode in the off-state. © *2009 American Institute of Physics*. [DOI: 10.1063/1.3156863]

Reversible resistive switching (RS) behavior in a metal-oxide-metal (MOM) sandwich structure has attracted a great deal of scientific and industrial interests due to the nonvolatile memory applications.[1–8] There are various RS behaviors when applying the electric field, including a bipolar,[1] unipolar,[2–8] and threshold switching.[9] Among them the unipolar RS mechanism has been intensively investigated due to the many advantages in the device operations.[3–8] A model based on the local conducting filament has been proposed, and explained the many features of the unipolar RS characteristics in terms of the formation and rupture of such conducting filaments within an insulative matrix. Since the unipolar RS operation was reported to show the strong material dependence,[2–8] exploring the unipolar RS mechanisms for various oxide materials would be important to seek the universal nature. In previous investigations as to unipolar RS, binary oxides including NiO,[2,3] TiO_2,[4,5] CuO,[6] and others[7,8] have been studied, and most of them have utilized the polycrystalline films. SnO_2 ($E_g \sim 3.5$ eV) is an abundant material and *n*-type semiconductor with oxygen vacancies.[10] The transport properties have been studied as transparent conducting oxides.[11] On the other hand there are no reports as to the RS characteristics of SnO_2 so far. From the viewpoint of the practical applications, the use of low temperature grown films is preferred to integrate the oxide materials with existing technologies. Thus these backgrounds motivated us to investigate the RS characteristics of room temperature grown SnO_2 thin films by fabricating the MOM structures.

SnO_2 thin films were grown on Pt/Ti/Si (100) substrate by pulsed laser deposition method (ArF eximer, $\lambda = 193$ nm). The film thickness was controlled to be 40 nm. Prior to the deposition of SnO_2 thin films, Pt as the bottom electrode was deposited onto the substrate with Ti buffer layer. The thickness of Pt bottom electrode was 100 nm. Oxygen pressure was controlled to be 10 Pa during the deposition of SnO_2 thin films. SnO_2 pellet target was used, which was obtained by sintering the milled SnO_2 powder (99.99% pure) at 1000 °C for 24 h. The laser power, the repetition rate, and the distance between the target and the substrate were set to be 40 mJ, 3 Hz, and 30 mm, respectively. The top electrode was then deposited onto the SnO_2 thin films by using a metal mask varying the area from $6.25 \times 10^2 (25 \times 25)$ μm^2 to $1.0 \times 10^4 (100 \times 100)$ μm^2. Note that all depositions of SnO_2 and Pt electrodes were performed at room temperature. X-ray diffraction (XRD) and high resolution transmission electron microscopy (HRTEM) (JEOL JEM-3000F) equipped with energy dispersed spectroscopy (EDS) were used to evaluate the crystal structure of the fabricated films. Current-voltage characteristics were evaluated using semiconductor parameter analyzer (Keithley 4200-SCS) at room temperature in the ambient atmosphere.

Figure 1(a) shows the XRD data of the SnO_2 thin film grown on the substrate. (111) oriented Pt bottom electrode can be seen in the figure. In addition, there were no observ-

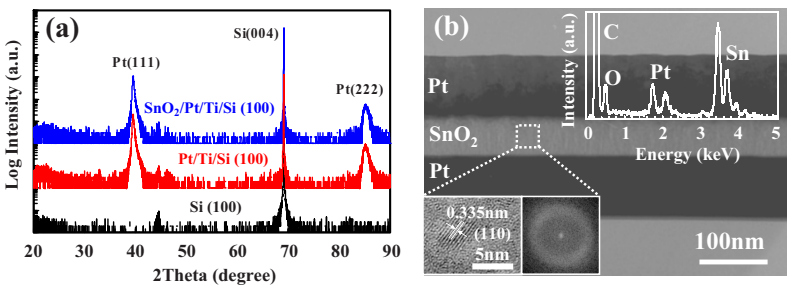

FIG. 1. (Color online) (a) XRD data of MOM structure. (b) Cross-sectional HRTEM image of SnO_2 thin film. The insets show the magnified image of HRTEM, the FFT diffractogram, and EDS data.

a)Electronic mail: yanagi32@sanken.osaka-u.ac.jp.
b)Electronic mail: kawai@sanken.osaka-u.ac.jp.

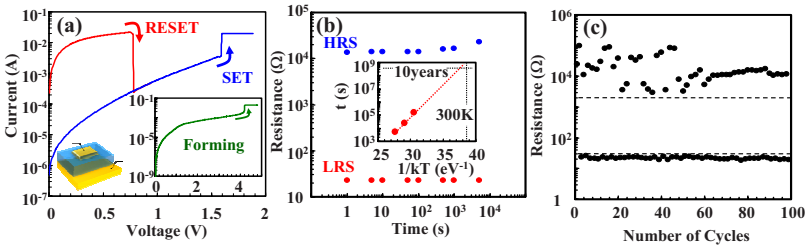

FIG. 2. (Color online) (a) Typical *I-V* data of the device structure. The inset shows the data of forming process. (b) and (c) show the retention and the endurance data of both LRS and HRS using the resistance data at 0.1 V. The inset of (b) shows the retention properties when varying the temperature. The lifetime was defined as the time when the resistance of LRS reached at the resistance value of HRS.

able peaks due to the presence of SnO_2 thin film. The microstructure of SnO_2 thin film was examined by HRTEM. The cross-sectional HRTEM images are shown in Fig. 1(b). The insets of Fig. 1(b) show the FFT diffractogram and the EDS data, which indicate the presence of Sn within the film. The film crystallinity seems to be amorphouslike phase, although there are partially crystalline nanoclusters less than 10 nm, which is fairly consistent with the XRD data. Figure 2(a) shows the typical *I-V* data of the device structure. The inset shows the data of forming process. The device showed the unipolar RS, which is in fact quite similar trend compared with existing devices using polycrystalline binary oxides.[2–8] The forming, set and reset processes typically occurred around 4–5, 1.5–2, and 0.5–1 V, respectively. Note that all our devices consistently exhibited such unipolar RS. Figure 2(b) and 2(c) show the retention and the endurance data by plotting the resistance data at 0.1 V. The low resistance on-state (LRS) and the high resistance off-state (HRS) were almost maintained in both the retention data over at least 10^4 s and the endurance data over 100 cycles. Note that the resistance of LRS state increased gradually with the time above 10^4 s due to the oxidization in atmospheric condition. To estimate the lifetime of the device, we examined the retention limit by varying the temperature in vacuum. The data is shown in the inset of Fig. 2(b). The lifetime was found to be over 10 year at 300 K. Thus the lifetime should be over 10 years in the presence of sealing layers. Thus observed RS phenomenon within room temperature grown SnO_2 thin film is nonvolatile.

Next we question what causes the nonvolatile RS effect on room temperature grown SnO_2 thin films. Previously, two major models including the Schottky barrier based-model and the conducting filaments based-model have been proposed.[2–8] In many previous reports as to the unipolar RS of polycrystalline binary oxides, the conducting filaments based-model has explained many features of unipolar RS characteristics.[2–8] The size dependence of the top electrode on the RS has been frequently utilized to probe the presence of local conducting filaments.[3] Figure 3(a) shows the size dependence of the top electrode on the *I-V* curves. There was no significant size dependence of the top electrode on both the on-state current and the reset current, inferring the presence of local conducting filaments. Assuming the presence of local conducting filaments, the distributions of the voltages for "set" and "reset" processes are closely related to the rupture and formation of local conducting filaments in previous "set" and "reset" process conditions. Note that as seen in Figs. 2 and 3, the voltages for "reset" processes for different conditions were found consistently around 0.8–1.1 V range. On the other hand, the voltages for "set" processes are ranged from 1.2 to 2.5 V and dependent on the conditions. The "set" voltage for 100×100 μm^2 electrode was less than that for 25×25 μm^2 electrode. This is possibly due to the probability of the formation of local conducting filaments near the anode, because the larger electrode might have more conducting filaments and also higher probability to connect the filaments with the electrode even under lower electric fields. Next, we examined the effect of top electrode material by using Pt, Au and Ti, in order to investigate the effect of the work functions of electrodes, i.e., Schottky barrier effect on the RS. In all top electrodes, the unipolar RS was consistently observed, although the Ohmic behavior was observed in both on- and off-states when using Au and Ti top electrodes, as shown in Figs. 4(a) and 4(b). Thus only the Schottky barrier based-model alone cannot rigorously explain the occurrence of the unipolar RS occurred within the present SnO_2 thin films. Furthermore, we examined the presence of the conducting filaments and the location of the RS by utilizing device structures comprised of two top electrodes and one bottom electrode as shown in the inset of Fig. 3(b). Figure 3(b) shows the *I-V* curves of the forming, set, and reset processes when applying the electric field between the two top electrodes. Note that the distance between the two top electrodes (50 μm) is long enough compared with the distance between the top electrode and the bottom electrode, i.e., the film thickness (40 nm). The forming voltage was nearly double of that in Fig. 2(a), and then the reset process was performed to obtain the off-state in the device structure. Two *I-V* curves of Fig. 3(c) shows the data between each top electrode and the bottom electrode after above reset process. The *I-V* curve for the top electrode, which was used as the cathode in the reset process in Fig. 3(b), showed the LRS, and the reset process occurred at the voltage around 0.8 V. On the other hand, the *I-V* curve for the top electrode, which was used as the anode in the reset process in Fig. 3(b), showed the HRS, and the set process occurred at the voltage around 1.1 V. Clearly these experi-

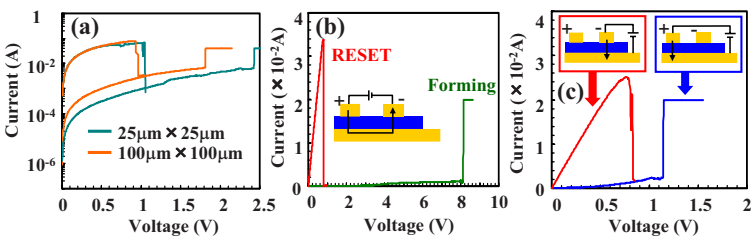

FIG. 3. (Color online) (a) Size dependence of the Pt top electrode on the *I-V* curves. (b) *I-V* curves of the forming, and reset processes when applying the electric field between the two Pt top electrodes. The inset shows the used device structure. (c) *I-V* curves between each top electrode and the bottom electrode after reset process.

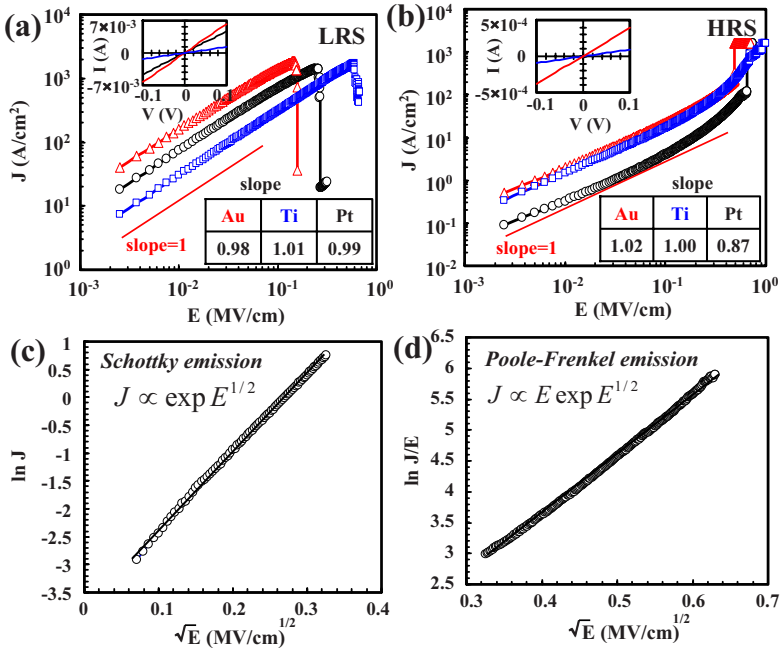

FIG. 4. (Color online) (a) LRS and (b) HRS data when using Pt, Au, and Ti top electrodes. (c) and (d) show the comparisons with Schottky emission model and Poole–Frenkel emission model, respectively.

mental results demonstrate the presence of the conducting filaments and the rupture and formation of such conducting filaments near the anode.

Next we analyzed the *I-V* curves of HRS and LRS when using Pt, Au, and Ti top electrodes to identify the transport properties of HRS and LRS. Figures 4(a) and 4(b) show the LRS and HRS data when using Pt, Au and Ti top electrodes. The Ohmic behavior of LRS was consistently observed for all top electrodes. Although the Ohmic behavior of HRS was observed when using Au and Ti, the Schottky behavior was observed for HRS when using Pt. Considering the work functions of the top electrodes [Pt(5.65 eV), Au(5.10 eV), Ti(4.33 eV)], the Ohmic behavior indicates the metallic state of LRS, which might be related to the metallic nature of $SnO_{2-\delta}$ ($\delta > 0.01$) due to the oxygen vacancies.[10] On the other hand, the Schottky behavior of HRS when only using Pt infers the presence of the Schottky barriers between Pt electrode and the insulating phase for HRS. The formula of Schottky emission model: $\ln J = \ln A^* T^2 - q(\phi_B - \sqrt{qE/4\pi\varepsilon})/k_B T$, in which J is the current density, E is the electric field, q is the electric charge, ε is the dielectric constant, k_B is Boltzmann's constant, T is the temperature, and A^* is the effective Richardson constant, can well describe the *I-V* data of HRS, which allows us to estimate the value of the Schottky barrier height to be 0.42 eV. Considering the work functions of top electrodes,[12] the bad gap, the electron affinity, and the activation energy of typical crystalline SnO_2,[13] the Schottky barrier height can be theoretically estimated to be about 0.4 eV, which is clearly close to the experimentally estimated barrier height of 0.42 eV. Thus these data highlight that the off-state local structure near the anode might be composed of insulative crystalline SnO_2. Above the Schottky barrier height of 0.42 eV, the *I-V* curves were well fitted by the formula of Poole–Frenkel emission model $\ln(J/E) \propto (\sqrt{q^3/\pi\varepsilon}/k_B T)\sqrt{E}$.[8] This indicates that the electron hopping between the trap states under high electric field governs the transport properties of insulative crystalline SnO_2 near the anode.

This work is partially funded by SCOPE.

[1] J. J. Yang, M. D. Pickett, X. Li, D. A. A. Ohlberg, D. R. Stewart, and R. S. Williams, Nat. Nanotechnol. **3**, 429 (2008).
[2] M.-J. Lee, S. I. Kim, C. B. Lee, H. Yin, S.-E. Ahn, B. S. Kang, K. H. Kim, J. C. Park, C. J. Kim, I. Song, S. W. Kim, G. Stefanovich, J. H. Lee, S. J. Chung, Y. H. Kim, and Y. Park, Adv. Funct. Mater. **19**, 1587 (2009).
[3] S. Seo, M. J. Lee, D. H. Seo, S. K. Choi, D.-S. Suh, Y. S. Joung, I. K. Yoo, I. S. Byun, I. R. Hwang, S. H. Kim, and B. H. Park, Appl. Phys. Lett. **86**, 093509 (2005).
[4] K. M. Kim, B. J. Choi, Y. C. Shin, S. Choi, and C. S. Hwang, Appl. Phys. Lett. **91**, 012907 (2007).
[5] S. C. Chae, J. S. Lee, S. Kim, S. B. Lee, S. H. Chang, C. Liu, B. Kahng, H. Shin, D.-W. Kim, C. U. Jung, S. Seo, M.-J. Lee, and T. W. Noh, Adv. Mater. (Weinheim, Ger.) **20**, 1154 (2008).
[6] K. Fujiwara, T. Nemoto, M. J. Rozenberg, Y. Nakamura, and H. Takagi, Jpn. J. Appl. Phys. **47**, 6266 (2008).
[7] H. Shima, F. Takano, H. Akinaga, Y. Tamai, I. H. Inoue, and H. Takagi, Appl. Phys. Lett. **91**, 012901 (2007).
[8] J. W. Seo, J.-W. Park, K. S. Lim, J.-H. Yang, and S. J. Kang, Appl. Phys. Lett. **93**, 223505 (2008).
[9] S. H. Chang, J. S. Lee, S. C. Chae, S. B. Lee, C. Liu, B. Kahng, D.-W. Kim, and T. W. Noh, Phys. Rev. Lett. **102**, 026801 (2009).
[10] H. Toyosaki, M. Kawasaki, and Y. Tokura, Appl. Phys. Lett. **93**, 132109 (2008).
[11] H. Kim and A. Piqué, Appl. Phys. Lett. **84**, 218 (2004).
[12] H. B. Michaelson, J. Appl. Phys. **48**, 4729 (1977).
[13] C. Körber, S. P. Hervey, T. O. Mason, and A. Klein, Surf. Sci. **602**, 3246 (2008).